

A statistical method of testing the gamma ray emission mechanisms of blazars

Xinyu Chi^{1*} and Enoch C.M. Young¹

Department of Physics and Materials Science, City University of Hong Kong, Tat Chee Avenue, Kowloon, Hong Kong

Received 11 October 1996 / Accepted 3 February 1997

Abstract. Models for generation of high energy gamma rays in blazars can be classified into two types of mechanisms in the jet comoving frame: relativistic electron scattering on the internal photons or magnetic field (virtual photons) (SIP) and on the external photons (SEP). These two mechanisms are known to result in a significant difference in the beaming effect. In this work, we propose a statistical test for the two types of mechanisms based on the beaming difference. The random variable is taken to be the K-corrected gamma ray to radio flux ratio and its distribution is shown to be a power-law with an index being model-dependent.

The feasibility of such a test is investigated with a limited sample of data which are compiled from the EGRET gamma ray survey, low resolution radio surveys and a VLBI radio survey. A correlation study indicates that the VLBI data are more suitable for the purpose than the low resolution data. Due to the limited amount of available data, the current test result is not statistically significant to discriminate the two emission mechanisms. Future generation of high energy gamma ray telescopes are needed to produce a larger sample of data of gamma ray blazars and their simultaneous observations with VLBI are called.

Key words: gamma rays: theory – galaxies: active – quasars: general – radiation mechanisms: nonthermal

1. Introduction

One of the most important discoveries by the Compton Gamma Ray Observatory is the detection of about 50 high energy gamma ray blazars by the EGRET instrument on board (Fichtel et al. 1994; Thompson et al. 1995). These sources have been identified as BL Lacs and Flat Spectrum Radio Loud Quasars (FSRQ). Some of them show optically violent variability and high polarization. The apparent gamma ray luminosity (assuming isotropic emission) of these sources are extremely high (up to 10^{49} erg s⁻¹) and may exceed the Eddington limit on the accretion power. Also rapid time variability (days) has been

seen in a number of blazars and this indicates the smallness of the gamma ray emission region. Therefore, relativistic jets are generally considered to be the emitting medium to boost the apparent luminosity and to fast the time variability (Blandford & Königl 1979; Marscher 1980; Königl 1981; Reynolds 1982).

A number of jet models have been proposed for the gamma ray emission from blazars. The popular ones include, synchrotron self-Compton (Ginzburg & Syrovatskii 1965; Rees 1967; Jones, O'Dell & Stein 1974; Maraschi, Ghisellini & Celotti 1992; Zdziarski & Krolik 1993; Bloom & Marscher 1996); and inverse Compton scattering on photons from the accretion disk (Dermer, Schlickeiser & Mastichiadis, 1992; Melia & Königl 1989); inverse Compton scattering on clouds-reprocessed photons (Sikora, Begelman & Rees 1994; Blandford & Levinson 1995); and synchrotron radiation by ultra-high energy electrons/positrons created in the ultra-high energy proton interactions (Mannheim 1993; Ghisellini 1993). Kinematically, these models can be divided into two classes: 1) relativistic electron scattering on internal photons or magnetic field, and 2) on external photons, in the jet comoving frame. Accordingly, the relativistic boosting effects are significantly different for these two cases (Dermer 1995).

One of the important characteristics of the gamma ray blazars is the presence of a strong core-dominated radio emission. Previous studies show that there is a moderate correlation between the gamma ray flux above 100 MeV and radio flux at 5 GHz, but no correlation between gamma ray flux and optical or X-ray flux (Dondi & Ghisellini 1995; Erlykin & Wolfendale 1995). The existence of the correlation indicates that the gamma ray emission is connected with the radio emission in blazars, either physically or kinematically. This can be understood in a way that the radio emission also emerges from the same jet and is thus Doppler-beamed to some extent. In this work, we use the radio flux as a reference to differentiate the beaming effect of gamma rays and to discriminate the emission models. In Sect. 2, we derive a beaming statistics for the jet models and show the theoretical difference in the the two classes of gamma ray emission mechanisms. In Sect. 3, we exemplify the test method with a limited sample of data. A correlation study is presented to show the link between the radio and gamma ray emission. Then we

Send offprint requests to: X. Chi

* Now at Department of Computer Science, Vanderbilt University, Nashville, TN37235, USA

perform the test with the limited sample of data. In Sect. 4, we verify the test method by examining various factors involved in the beaming statistics with Monte-Carlo simulations. The effects of the random spreads in the relevant parameters on the test result are estimated. Finally, in Sect. 5, we discuss the need for simultaneous observations of VLBI with high energy gamma ray telescopes to produce a larger, better quality sample of data.

2. A beaming statistics

The kinematic effect of a relativistically moving jet can be characterized by the Doppler factor

$$\delta = [\gamma(1 - \beta \cos \theta)]^{-1} \quad (1)$$

where β is the speed of the jet flow in units of the speed of light, γ is the Lorentz factor and θ is the angle between the observer and the axis of jet. The relativistic Doppler effect on the radiation from the jet is beaming and boosting, i.e. the superluminal effect. The relation between the luminosity L in the observer's frame and the intrinsic luminosity L_0 in the rest frame of jet can be quantified through the Doppler factor δ ,

$$L = \delta^{\eta+\alpha} L_0 \quad (2)$$

where α is the power law index of the differential energy spectrum of the radiation. η is a geometrical parameter, $\eta = 3$ for point sources and $\eta = 2$ for one-dimensional continuous sources (e.g. Lind & Blandford 1985). Here the coefficient $B = \delta^{\eta+\alpha}$ is defined as beaming factor. The above relation is valid only for the case in which both the projectiles and targets are assumed to be isotropic in the jet comoving frame.

For the case in which the isotropic target photons (in the observer's frame) are external to the jet comoving frame, Dermer (1995) has derived the beaming factor for a blob (point source) in which gamma rays are produced via inverse Compton scattering,

$$B = \delta^{\eta+2\alpha_g} \quad (3)$$

where α_g is the gamma ray energy spectral index and the average observational value is about 1.0; and η takes a larger value $\eta = 4$. It can be seen clearly that the beaming effect is more dramatic than the previous case. There is also an angular factor $(1 + \cos \theta)^{1+\alpha}$ in the Dermer's formulation. We neglect it in our formulation for simplicity. It is useful to mention that the beaming factor is still of the same order of magnitude if the external photons are not isotropic. For example, for the case of external photons coming from the accretion disk, Dermer, Schlickeiser and Mastichiadis (1992) have demonstrated the beaming factor to be δ^{3+s} where s is the spectral index of relativistic electrons and their preferred value is 3 (cf. the canonical value of α_g is 1). The effect caused by anisotropy in the external photon field is just a different angular profile of the gamma ray beams.

Now we use the difference in beaming effect to discriminate between the two classes of gamma ray emission models, statistically. First of all, we need to specify the key parameter which enables the theoretical models to be related to the

observed statistics. The parameter is the index in the beaming factor, specifically the power-law index of radiation spectrum. Observationally, radio and gamma ray emissions have different indices and thus their flux ratio will retain the Doppler factor. Then we choose the K-corrected flux ratio of gamma ray to radio as the random variable to formulate our statistical test. The radio emission is generally believed to be synchrotron emission along the jet and its beaming factor is thus fixed. We consider only a special combination of emission characters in which gamma ray emission is from a moving blob and radio emission is from a continuous jet. This choice is consistent with some theoretical models of gamma ray emission (e.g. Ghisellini & Madau 1996; Böttcher, Mause & Schlickeiser 1996). The results from simultaneous multiwavelength observations of gamma ray blazars 3C 273 (Lichti et al. 1995) and 3C 279 (Hartman et al. 1996) show little time variability in radio emission and no radio flares co-occurring with gamma ray flares. Thus we may conclude that the radio emission in blazars is from a continuous jet rather than from a moving blob. It might not hold for the radio cores seen by VLBI. Other combinations can be formulated in a similar way.

Two assumptions are made here to simplify the formulation. The first one is that there is a proportionality between the intrinsic luminosities of gamma ray and radio emission in blazars, and that its dispersion is small. The second one is the same Lorentz factor γ for both gamma ray and radio emissions of all blazars. The observational justification and theoretical argument will be made later in Sect. 4. With these two assumptions, we define x to be the observed flux density ratio of gamma ray f_g to radio f_r (after the K-corrections) and thus x is approximately proportional to the beaming factor ratio of gamma ray to radio,

$$x = \frac{f_g}{f_r} \propto \delta^a \quad (4)$$

where $a = \eta_g - \eta_r + n\alpha_g - \alpha_r$ and depends on the gamma ray models. For our choice of radio emission model, $\eta_r = 2$. For the SIP gamma ray model, $\eta_g = 3$ and $n = 1$. For the SEP gamma ray model, $\eta_g = 4$ and $n = 2$.

For a fixed γ , δ is the sole function of $\cos \theta$ as defined in Eq. (1). So is x . Here we ascribe the variation of δ^a to the change in $\cos \theta$. If a gamma ray emitting jet is isotropically oriented in 3-dimensional space, i.e. $\cos \theta$ is uniformly distributed, it is easy to derive the distribution of δ^a which follows a power law (e.g. Urry & Shafer 1984; Chi & Young 1996),

$$g(\delta^a) \sim (\delta^a)^{-\frac{a+1}{a}} \quad (5)$$

A power law distribution has the property of scaling-invariance with respect to its variable. As $x \propto \delta^a$, we have the same power law distribution for x

$$g(x) \sim x^{-\frac{a+1}{a}} \quad (6)$$

The index $(a+1)/a$ depends on the model of gamma ray emission. For the choice of $\alpha_g = 1.0$ and $\alpha_r = 0.0$, it equals 1.5 for the SIP model and 1.25 for the SEP model. If the angular

factor $(1 + \cos \theta)^{1+\alpha}$ is included in the SEP model, the index will become even smaller and thus the index difference between the two models will become larger. As argued by Dermer (1995), the effect of this angular factor is relatively small and thus can be neglected in our formulation.

3. A pilot test with the current data

The only available data for the gamma ray fluxes of blazars are those given in the Second Catalog of High Energy Gamma Ray Sources compiled by the EGRET team (Thompson et al. 1995). The relevant quantities include the gamma ray number flux above 100 MeV and the power law spectral index. Since many sources are time variable and observations at different viewing periods give different fluxes and spectral indices, we average the fluxes and indices for each source with a weighting factor being proportional to the photon number recorded in each period. Then we convert the photon number flux integrated above 100 MeV into the differential energy flux at 100 MeV, assuming a single power spectrum in the energy range 100 MeV - 10 GeV. For those sources whose spectral indices are not given in the Catalog, we assume that the differential number indices are 2.0 or the differential energy indices are 1.0 in our analysis.

We have compiled two sets of radio data for the gamma ray blazars. One is from the all-sky low resolution surveys at 5 GHz (Kühr et al. 1981; Becker, White & Edwards 1991; Gregory & Condon 1991). The relevant quantities include the radio flux density at 5 GHz and power law spectral index between 2.7 GHz and 5 GHz. The other is from the all-sky VLBI survey at 2.3 GHz (Preston et al. 1985). The relevant quantity is the “correlated” flux density defined by the authors. Cosmological redshifts are needed for the K-correction in our analysis, and the data are taken from the Quasar Catalog of Hewitt and Burbidge (1993). For those blazars without z measurements, we simply assign $z = 1.0$.

Table 1 lists our sample of data. Column 1 gives the name of the sources in terms of celestial coordinates (1950); column 2 gives the redshifts; column 3 gives the integrated gamma ray number fluxes above 100 MeV in units of $10^{-6}\text{cm}^{-2}\text{s}^{-1}$; column 4 gives the indices of differential gamma ray energy spectra; column 5 gives the radio flux densities at 5 GHz; column 6 gives the radio spectral indices between 2.7 GHz and 5 GHz; and column 7 gives the radio flux densities from the VLBI survey at 2.3 GHz. The radio flux densities are in units of Jy.

We start our analysis with a correlation study of the sample of data. Fig. 1 shows the scatter plot of radio spectral index α_r versus gamma ray spectral index α_g . Here α_r is defined in such a way that $f_r \propto \nu^{-\alpha_r}$ where ν is the radio frequency. There are totally 31 datum points. The Pearson’s r is calculated and is found to be $r = 0.3245$ and the corresponding probability of confidence is $1 - 3.74 \times 10^{-2}$. Therefore, the correlation is moderately significant. The interpretation of such a correlation is not straight forward as the radio emission is generally believed to be a superposition of synchrotron radiations emerging from different parts of an inhomogeneous source (jet) in which synchrotron self-absorption plays a role. The radio index may

Table 1. The data sample. Column 1 – the name of the sources in terms of celestial coordinates (1950); column 2 – the redshifts; column 3 – the integrated gamma ray number fluxes above 100 MeV in units of $\text{cm}^{-2}\text{s}^{-1}$; column 4 – the indices of differential gamma ray energy spectra; column 5 – the radio flux densities at 5 GHz in Jy; column 6 – the radio spectral indices between 2.7 GHz and 5 GHz; and column 7 – the radio flux densities from the VLBI survey at 2.3 GHz in Jy.

Name	z	F_g	α_g	f_r	α_r	f_{rc}
2356+196	1.07	0.21		0.71	0.20	0.38
0202+149	1.20	0.25	1.5	2.47	-0.43	0.60
0208-512	1.00	0.91	0.7	3.31	-0.12	2.23
0235+164	0.94	0.63	0.9	2.85	1.03	1.80
0420-014	0.92	0.28	0.9	1.46	0.01	0.61
0446+112	1.21	0.35	1.1	1.23	-0.56	0.20
0521-365	0.06	0.20	1.2	9.30	0.45	0.99
0528+134	2.06	1.05	1.3	3.98	-0.47	0.50
0537-441	0.89	0.22	1.0	4.00	-0.06	2.03
0716+714	0.30	0.20	0.9	1.12	-0.22	0.11
0735+178	0.42	0.15		1.99	-0.05	0.60
0827+243	2.05	0.25		0.86	-0.23	0.80
0829+046	0.18	0.19				0.32
0836+710	2.17	0.17	1.4	2.59	0.33	0.37
0954+556	0.90	0.08		2.28	0.19	0.10
0954+658	0.37	0.11	0.9	1.46	-0.35	0.43
1101+384	0.03	0.17	0.7	0.64	0.25	0.32
1127-145	1.19	0.43		6.75	0.03	1.49
1156+295	0.73	2.30	1.0	1.5	0.40	0.43
1222+216	0.44	0.26	1.1	0.97	0.40	0.33
1226+023	0.16	0.18	1.5	42.9	-0.15	1.51
1229-021	1.05	0.12		1.07	0.29	0.09
1253-055	0.54	1.90	0.9	15.0	-0.30	3.70
1331+170	2.08	0.09		0.54	-0.49	0.21
1406-076	1.49	0.82		1.30	-0.20	0.64
1510-089	0.36	0.25	1.3	3.08	-0.31	2.30
1604+159		0.24	1.0	0.50	0.30	
1606+106	1.23	0.39	1.3	1.49	-0.42	0.49
1611+343	1.40	0.39	0.9	2.67	-0.11	1.20
1622-253		0.35	1.3	2.08	0.14	0.15
1633+382	1.81	0.83	1.0	4.02	-0.73	1.30
1730-130	0.90	0.39	1.4	0.22	0.10	1.42
1739+522	1.38	0.30	1.2	1.98	-0.08	0.65
1908-201		0.19	1.5			0.46
1933-400	0.97	0.24	1.4	1.48	-0.26	0.28
2052-474	1.49	0.19	1.4	2.52	0.11	0.38
2209+236		0.13				0.55
2230+114	1.04	0.28	1.6	3.61	0.50	0.60
2251+158	0.86	0.84	1.2	17.4	-0.64	3.40
0130-171	1.02	0.13		1.00	0.06	0.27
0219+428	0.44	0.17	0.9	0.92	0.00	0.27
0234+285	1.21	0.17	1.7	1.44	0.24	1.60
0458-020	2.29	0.16		1.74	0.08	0.92
0804+499	1.43	0.13		2.05	-0.47	0.57
0805-077	1.84	0.30	1.4	1.04	0.32	0.74
0917+449	2.18	0.14	0.9	1.00	0.20	0.12
1317+520	1.06	0.10		0.16	0.50	
1313-333	1.21	0.22	0.8	1.36	-0.50	0.82

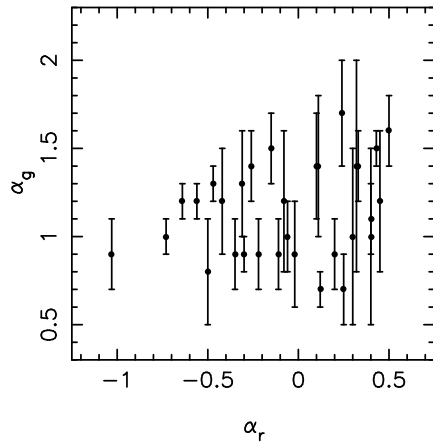


Fig. 1. The scatter plot of the index of differential energy spectra of gamma ray emission versus that of radio emission for 31 blazars detected by the EGRET instrument on board CGRO. There is a moderately significant correlation with probability $1 - 3.75 \times 10^{-2}$.

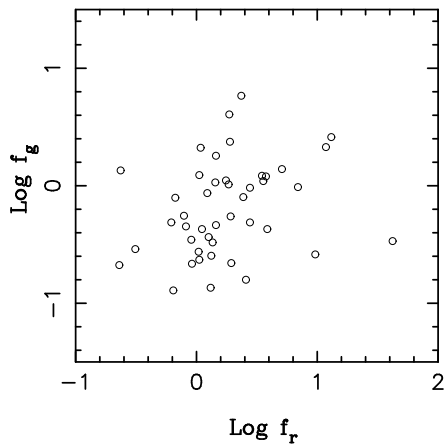


Fig. 2. The scatter plot of the flux density of gamma ray emission at 100 MeV versus the low resolution flux density of radio emission at 5 GHz for 44 blazars. Both fluxes are K-corrected. The gamma ray flux density is in units of $10^{-6} \text{ MeVcm}^{-2}\text{s}^{-1}\text{MeV}^{-1}$; and the radio one is in units of Jy. A moderately significant correlation is found with probability $1 - 4.43 \times 10^{-2}$.

be understood as a measure of the degree of inhomogeneity in the emission region.

Next, we study the correlation between radio fluxes and gamma ray fluxes. The integrated gamma ray number fluxes are converted into differential energy fluxes at 100 MeV. The K-correction $(1+z)^{\alpha-1}$ is made for both the gamma ray and radio flux densities. For those gamma ray sources without z measurement, we assume that $z = 1.0$; and for those without α_g , we assume that $\alpha_g = 1.0$. In Fig. 2, the gamma ray flux density f_g is plotted versus the radio one f_r of low resolution. The former is in units of $10^{-6} \text{ MeVcm}^{-2}\text{s}^{-1}\text{MeV}^{-1}$ and the latter is in units of Jy. There are totally 44 datum points. The Pearson's r turns out to be $r = 0.2598$ and the corresponding probability is $1 - 4.43 \times 10^{-2}$. It is consistent with the result

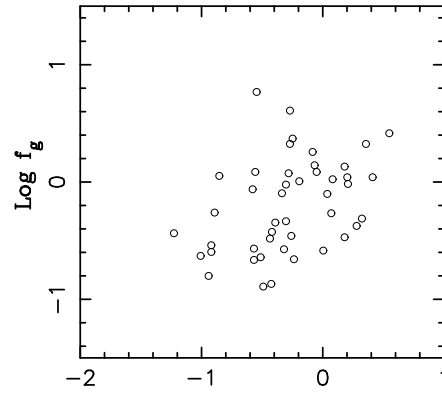


Fig. 3. The scatter plot of the flux density of gamma ray emission at 100 MeV versus the VLBI flux density of radio emission at 2.29 GHz for 45 blazars. Both flux densities are K-corrected. The gamma ray flux density is in units of $10^{-6} \text{ MeVcm}^{-2}\text{s}^{-1}\text{MeV}^{-1}$; and the radio one is in units of Jy. A more significant correlation is found with probability $1 - 3.64 \times 10^{-3}$.

of Dondi & Ghisellini (1995). The significance of this result is moderate and it may be interpreted as evidence for a kinematical link between the gamma ray and radio emission in blazars, i.e. both of the emissions are boosted by the relativistic Doppler effect.

In Fig. 3, we plot the gamma ray flux density f_g versus the radio one f_{rc} of high resolution (VLBI survey). These flux densities are also K-corrected with the above procedure. There are totally 45 datum points. The correlation is found to become stronger, with $r = 0.3978$ and the probability of confidence $1 - 3.64 \times 10^{-3}$. This more significant correlation strengthens our view that the gamma ray and radio emission are kinematically linked. The radio core flux is normally a small fraction of the total and it may emerge only from a specific part of the jet. Further, it is likely that the gamma ray emission in blazars emerges from the radio core where the Lorentz factors for both emissions are equal or very close in value. The deviations from the correlation are due to the random spreads in the intrinsic luminosity ratio, spectral index and Lorentz factor. These effects will be studied with Monte-Carlo simulations in Sect. 4. We may conclude that the VLBI data are more suitable for the test of beaming statistics.

Now let us perform the test with our sample of data. The observed distribution of x is made from our sample data of 45 blazars in which the radio data are taken from VLBI surveys. For those blazars without α_r measurement, we take 0.0 for it. Similarly, for those without α_g , we take 1.0 for it. The distribution is shown in Fig. 4 where the data are binned into 5 intervals on logarithm-logarithm scales. The errors are purely statistical one. A least-square fit to the 5 points gives the power law index (slope) 1.42 ± 0.20 . If we remove the two end points, a least-square fit to the 3 points in the middle leads to 1.45 ± 0.24 for the index. In the next section, we will show that these three points are governed by the beaming effects while the two end

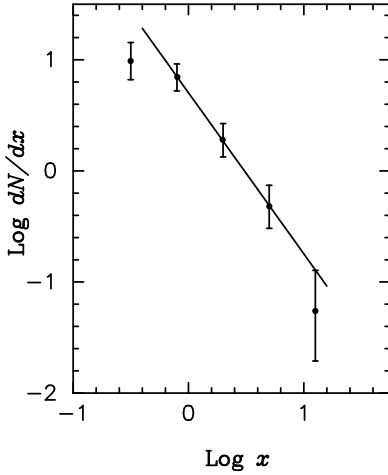


Fig. 4. The distribution of the ratio of gamma ray flux density to radio one. Both flux densities are K-corrected. The units used are the same as those in Fig. 2 and Fig. 3. The errors given are purely statistical. The three middle points align right on a straight line and a least-square fit gives a slope 1.45 ± 0.24 .

points are produced by other effects. The significance of the test result is not high enough to rule out any model.

4. Verification of the method

In the system of a gamma ray emitting jet, many physical processes occur at the same time and a large number of quantities are needed to give a full description of the gamma ray emission. Some of the physical processes are inter-related and the corresponding quantities are inter-dependent. Further, the physical conditions may vary from jet to jet to a certain extent and the same quantity may take different values for different jets. In formulating the above beaming statistics, we have made a few assumptions to simplify the derivation of the x -distribution and successively the test with a sample of data. The validity of these assumptions are needed to be verified. Also the effects of random spreads in the physical quantities on the final x -distribution should be examined. In this section we will show that all these effect are minor compared to the beaming effect and that the x -distribution is mainly governed by the beaming effect.

4.1. Monte-Carlo Simulations of the flux correlation

To demonstrate our interpretation that the flux correlation is largely due to the co-axially Doppler beaming effect, we used Monte-Carlo simulations to generate the beamed gamma ray and radio fluxes. To make the problem simpler, we assume that the standard-candle sources are homogeneously located in an Euclidean space and thus the distribution of intrinsic fluxes obeys the well-known power law $f^{-5/2}$. We sample the intrinsic fluxes according to this power law and multiply them with a beaming factor. The beaming factor, as defined in Sect. 2, is a function of multi-variables which include the emission region geometry factor η , emission spectral index α , the Lorentz factor

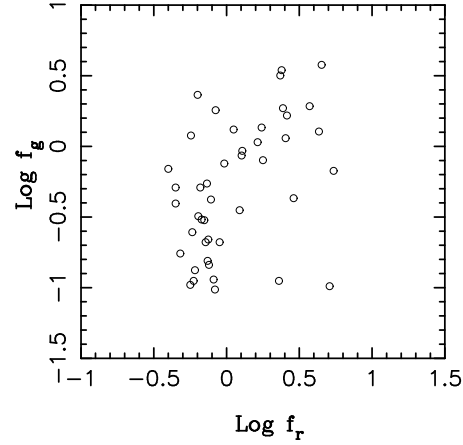


Fig. 5. A Monte-Carlo sample of data of gamma ray and radio flux densities. There are totally 44 datum points. The gamma ray and radio intrinsic luminosities are uncorrelated, but both are boosted with the same Lorentz factor and their spectral indices are fixed. A significant correlation is created at a confidence level $1 - 2.0 \times 10^{-3}$.

γ and the viewing angle θ . In the Monte-Carlo simulations, we will always treat θ as a random variable distributed isotropically in 3-dimensional space and set its range to $0^\circ - 7^\circ$. The η s will be taken to be fixed values. But the γ or α will be treated as fixed parameter in some cases and as random variable in other cases. In the following we study three typical cases.

(1). The intrinsic gamma ray and radio emissions are uncorrelated, but both are boosted with the same Lorentz factor and their spectral indices are fixed. The intrinsic fluxes of gamma rays and radio are sampled from the power law distribution $f^{-5/2}$, respectively. Their variation ranges are set to be two decades. $\cos\theta$ is sampled from a uniform distribution. γ is set to 10.0. α is taken to be 1.0 for gamma rays and 0.0 for radio. Also η is taken to be 3.0 for gamma rays and 2.0 for radio. The sample size is 44 which is about the same as that of the observed one. Fig. 5 displays a sample of Monte-Carlo data which is one of the least correlated cases. A correlation study is made of the Monte-Carlo samples and the Pearson's r is used to measure the significance. The confidence level for the existence of a correlation is $1 - 2.0 \times 10^{-3}$. This indicates that only the co-axial beaming can make two uncorrelated emissions become correlated. If a straight line is fitted to the data, the slope is about 2.0.

(2). The intrinsic gamma ray and radio emissions are in exact proportion in each blazar, but the Lorentz factor varies from blazar to blazar. The energy (frequency) spectral indices are fixed. The intrinsic flux of gamma rays is sampled from the power law distribution $f^{-5/2}$ and the radio one is obtained by scaling it. Their variation ranges are set to one decade. $\cos\theta$ is sampled from a uniform distribution. α is taken to be 1.0 for gamma rays and 0.0 for radio. We take the Lorentz factor γ as random variable and assume that $\log\gamma$ obeys a Gaussian distribution with a mean 1.0 and a standard deviation 0.477 for both gamma ray and radio emission. Fig. 6 displays a sample

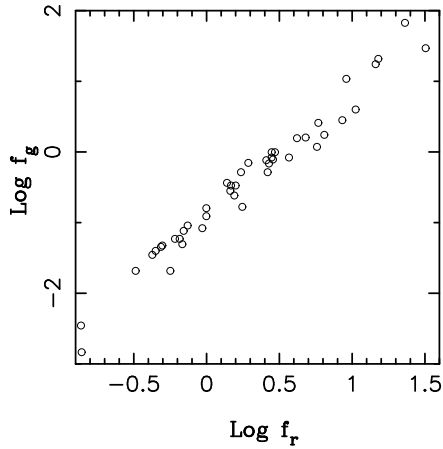


Fig. 6. A Monte-Carlo sample of data of gamma ray and radio flux densities. There are totally 44 datum points. The intrinsic gamma ray and radio emissions are in exact proportion in each blazar, but the Lorentz factor varies from blazar to blazar. The energy (frequency) spectral indices are fixed. The slope of the regression line (on logarithm-logarithm plot) has been altered from 1.0 to about 2.0.

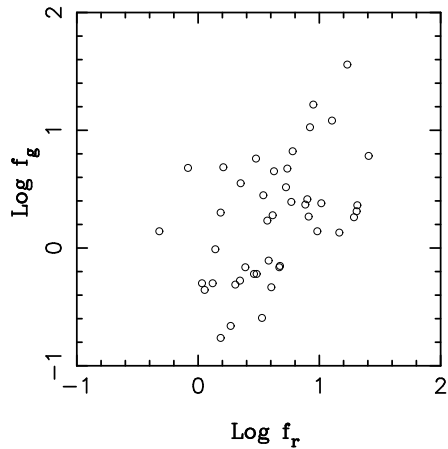


Fig. 7. A Monte-Carlo sample of data of gamma ray and radio flux densities. There are totally 44 datum points. The intrinsic gamma ray and radio emissions are in exact proportion and a fixed Lorentz factor $\gamma = 10$ is set for both, but their energy (frequency) spectral indices are independent random variables. The strong correlation is retained at a confidence level $1 - 5.0 \times 10^{-4}$ but the slope has been changed from 1.0 to about 2.0.

of Monte-Carlo data which comprise 44 points. Clearly, we can see that the tight correlation between the two fluxes has been preserved but the slope (on logarithm-logarithm plot) has been altered from 1.0 to about 2.0. The former slope is set by our assumption and the latter one is ruled by the difference in the beaming effects of the radio and gamma rays.

(3). The intrinsic gamma ray and radio emissions are in exact proportion and a fixed Lorentz factor $\gamma = 10$ is set for both, but their energy (frequency) spectral indices are independent random variables. The indices are assumed to follow Gaussian distributions with a standard deviation 0.3. The mean is set to 1.0

for gamma rays and 0.0 for radio. The intrinsic flux of gamma rays is sampled from the power law distribution $f^{-5/2}$ and the radio one is obtained by scaling it. Their variation ranges are set to one decade. $\cos\theta$ is sampled from a uniform distribution. Fig. 7 displays a sample of Monte-Carlo 44 datum points. This sample is one of the most severely smearing cases, and the existence of a correlation has a high confidence level $1 - 5.0 \times 10^{-4}$ by the Pearson's r . The strong correlation is retained and the slope has been changed to about 2.0. If the gamma ray index is correlated with the radio one, we may expect an even stronger correlation.

All the three cases show that the co-axial beaming effect plays the dominant role in making the correlation between gamma ray and radio emission for a reasonably large Lorentz factor (~ 10). The slope of the regression line is dictated by the differential beaming effect, i.e. the difference in gamma ray beaming and radio beaming. Therefore, we can draw the conclusion that the observed correlation between the EGRET gamma ray flux and the VLBI radio flux is largely due to the co-axial beaming effect. The dispersion in the correlation can be attributed to the spreads in the Lorentz factors and energy spectral indices, as well as in the proportionality between intrinsic gamma ray and radio luminosity.

4.2. Deviations in the x -distribution

In Sect. 2, we demonstrate that the x -distribution is a perfect power law if x is solely a function of the viewing angle θ while other parameters in the expression Eq. (4) remain constant. However, there are actually random spreads in these parameters and one would expect a deform in the x -distribution. The x function can be divided into two parts, one is the intrinsic flux ratio of gamma ray to radio, and the other is the Doppler beaming factor ratio. Let us look at the beaming part first. Previously, the effect of a spread in the Lorentz factor on the apparent luminosity function (a power law function of the Doppler factor) has been examined by Urry and Padovani (1991). In the presence of the beaming effect, the apparent luminosity function turns from a single power law into a double power law. These authors show that the spread does not affect the indices of the two power laws but just makes the index transition smoother. That is, the random spread deforms only the end parts of a power law distribution.

The effect of a random spread in the energy/frequency spectral indices of gamma rays and radio on the beaming part of the x -distribution is negligible. This is because the index of the x -distribution is a quotient function of the spectral indices and it is insensitive to any variation in the spectral indices. Let us show it analytically. The variation of the index $(a + 1)/a$ of x can be derived in terms of its variable a ,

$$\Delta \left(\frac{a + 1}{a} \right) = - \frac{\Delta a}{a^2} \quad (7)$$

where a contains the energy spectral indices α as defined in Sect. 2. Observations indicate that the variation of the energy spectral index is much less than a , i.e. $\Delta a \ll a$. Thus we have

$\Delta[(a+1)/a] \sim 0$ for the case $a > 1$. In other word, the x -distribution is not largely affected by the spreads in the energy spectral indices. Of course, we may expect a deform in the end parts of the distribution.

Now turning to the part of flux ratio, we examine the random spread in it. In Sect. 2, we simply treat the flux ratio as a constant. This is a strong assumption and thus needs justification. Physically, whether the gamma ray and radio emissions are linked is not very clear but depends on model. Nevertheless, we may put forward a scaling argument in which both emissions are roughly proportional to the accretion power in a blazar. However, the random spread in it cannot be given by the argument. Here we take an empirical approach and determine the spread magnitude from the observational data.

Let us define y to be the intrinsic flux ratio and assume that its logarithm obeys a Gaussian distribution with a standard deviation σ , i.e.

$$g(\log y) \sim e^{-\frac{\log y}{2\sigma^2}} \quad (8)$$

Here the flux units are chosen in such a way that the mean of the distribution is 0. The distribution of y can be derived from the above equation,

$$h(y) = g(\log y) \frac{d\log y}{dy} = y^{-\left(\frac{\log y}{2\sigma^2 \ln 10} + 1\right)} \quad (9)$$

If we take logarithm on the both sides, a parabola appears as

$$\log h(y) = -\frac{\log^2 y}{2\sigma^2 \ln 10} - \log y \quad (10)$$

which is symmetrical about a vertical line.

If we define the reciprocal of y as $t = y^{-1}$, then t obeys the same distribution as y . This can be derived through the relation $\log t = -\log y$ which obeys the same Gaussian distribution as $\log y$. Therefore we conclude that the distributions of y and its reciprocal are the same parabola on logarithm-logarithm plot. We will use this symmetrical property to justify either the flux ratio or the beaming ratio dominates the observed x -distribution. The logic is following. If we take the two ratios as random variables, then their product x is also a random variable. The distribution of x is solely determined by those of the ratios'. It has a simple property that it is spanned by the two sub-distributions over a wider range and has a convex shape. For example, if one of sub-distribution is a power law, the product distribution is a power law in the middle part and attached with other shapes at the end parts.

The distribution of the observed x^{-1} is made from our sample of data and is shown in Fig. 8. If the dispersion in y is large, the x -distribution will be dominated by the y -distribution and thus have the symmetrical property as indicated above. Otherwise, the distribution will be dominated by the power law of the beaming factor ratio. Comparison of Figs. 4 and 8 clearly show a difference between these two distributions. The slope of linear fit to the three middle points in Fig. 8 is 0.55 ± 0.29 . The three middle points are well on the power law lines in both cases and

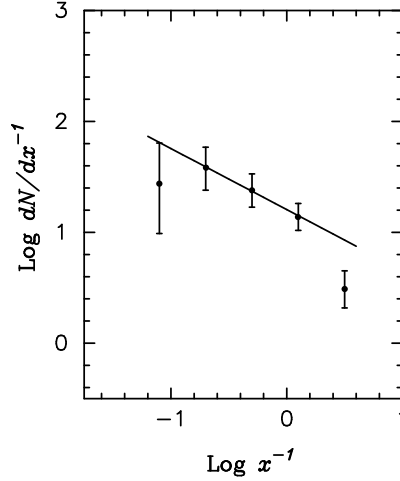


Fig. 8. The distribution of the flux density ratio of radio to gamma ray one, i.e. the reciprocal of x . Both flux densities are K-corrected. The errors given are purely statistical. The three middle points align right on a straight line and a least-square fit gives a slope 0.55 ± 0.29 .

therefore the power law dominates the observed distribution. If we attribute the deform at the end parts entirely to the dispersion in y , the dispersion in logarithm is about 0.3 which corresponds a factor 2 on linear scale.

Unless the theoretical distribution of y obeys the same power law as that of the beaming factor ratio, the distinction can always be made. It is more likely that y obeys a Gaussian than a specific power law. Although no exact emission model predicts this argument, some physical justification can be made. It is generally agreed that the gamma rays and radio are produced by different populations of relativistic electrons. If there is any physical link between these populations of electrons, it must be indirect. In the mean time, many processes are involved in the link and the accumulated dispersions naturally obeys a Gaussian.

5. Discussion and conclusions

In our sample of data, the gamma ray and VLBI radio flux were not measured simultaneously. This non-simultaneity may introduce a further random spread in the gamma ray – radio correlation and in the x -distribution. It is known that some of the gamma ray blazars are highly time variable. The gamma ray fluxes used here are the *averaged* over a period of time of two weeks, albeit the sampling of the high and low state may not be even. The VLBI radio fluxes are the *instant* in the sense that the observation time for a source is about one hour but the time variability of large amplitude (a few ten percent) in radio is at least days. Therefore, simultaneous observations of VLBI with gamma ray telescopes are needed to yield “average” radio fluxes for the beaming statistics.

Furthermore, such simultaneous observations are also useful in studying the correlation between radio and gamma ray emissions. Some blazars are found to have intraday variability throughout the entire electromagnetic radiation spectrum (see

review by Wagner & Witzel 1995). It will be interesting and important to look at the time profiles of radio and gamma ray emission simultaneously for a specific blazar. If a good correlation is found, there must be an underlying physical link between the two emission mechanisms. If there is a time lag, there should be also a physical link which might be more indirect. Otherwise, the apparent flux correlation of moderate significance seen in Sect. 3 has to entirely result from the co-axial relativistic Doppler beaming.

In conclusion, we propose a statistical test for the gamma ray emission mechanisms in blazars in this work. It is based on the difference in the relativistic Doppler effects of gamma ray emission models, specifically inverse Compton scattering on internal photons and on external photons. The radio flux from blazar is believed to be Doppler beamed too and thus utilized as a reference to differentiate the beaming effect. The K-corrected flux ratio of gamma ray to radio x is taken to be the random variable and its distribution is derived as a power law with the index being model-dependent. A test with the currently available data gives a result of only 1σ significance and a firm discrimination between the two models cannot be made. The next generation of high energy gamma ray telescopes, such as GLAST, are needed for producing a larger sample of data to give a more significant test result.

A justification of the method has been made and it is proved to be feasible for the purpose of testing the gamma ray emission mechanisms. A correlation study of gamma ray and radio data indicates that high resolution VLBI data are more suitable than low resolution data. Our Monte-Carlo simulations show that the observed correlation between gamma ray and radio flux could be purely due to the co-axial beaming effect though a physical link is a plus. The random spreads in the parameters of the Doppler factor are examined and their effect on the x -distribution is verified to be minor. The assumption of a fixed ratio of gamma ray to radio intrinsic emission is validated and the random spread associated with the ratio is proved to be small. Simultaneous observation of VLBI with gamma ray telescopes are needed to provide a better quality sample of data for the x -distribution and for exploring a physical link between the gamma ray and radio emission in blazars.

Acknowledgements. The authors wish to thank Prof. Y.Y. Zhou for helpful suggestions. The anonymous referee is acknowledged for useful comments. The EGRET team are kindly thanked for their great effort in preparing the Catalogs of High Energy Gamma Ray Sources. This work is supported by a Strategic Research Grant of the City University of Hong Kong.

References

- Becker, R.H., White, R.I. & Edwards, A.L. 1991, ApJS 75, 1
 Blandford, R.D., & Königl, A. 1979, ApJ 232, 34
 Blandford, R.D., & Levinson, A. 1995, ApJ 441, 79
 Bloom, S.D., & Marscher, A.P. 1996, ApJ 461, 657
 Böttcher, M., Mause, H., & Schlickeiser, R. 1996, A&A submitted
 Chi, X., & Young, E.C.M. 1996, J. Phys. G submitted
 Dermer, C. 1995, ApJ 446, L63
 Dermer, C., Schlickeiser R., & Mastichiadis, A. 1992, A&A 256, L27
 Dondi, L., & Ghisellini, G. 1995, MNRAS 273, 583
 Erlykin, A.D., & Wolfendale, A.W. 1995, J.Phys.G, 21, 1149
 Fichtel, C.E., et al. 1994, ApJS 94, 551
 Ghisellini, G. 1993, Adv. Space Res., 13, 587
 Ghisellini, G., & Madau, P. 1996, MNRAS 280, 67
 Ginzburg, V.L., & Syrovatskii, S.I. 1965, ARA&A, 3, 297
 Gregory, P.C., & Condon, J.J. 1991, ApJS 91, 111
 Hartman, R.C., et al. 1996, ApJ 461, 698
 Hewitt, A. & Burbidge, G. 1993, ApJS 87, 451
 Jones, T.W., O'Dell, S.L., & Stein, W.A. 1974, ApJ 188, 353
 Königl, A. 1981, ApJ 243, 700
 Kühn, H., Witzel, A., Pauliny-Toth, I.I.K., & Nauber, N. 1981, A&AS 45, 367
 Lichti, G.G., et al. 1995, A&A 298, 711
 Lind, K.R. & Blandford, R. D. 1985, ApJ 295, 358
 Mannheim, K. 1993, A&A 269, 67
 Maraschi, L., Ghisellini, G., & Celotti, A. 1992, ApJ 397, L5
 Marscher, A. P. 1980, ApJ 235, 386
 Melia, F., & Königl, A. 1989, ApJ 340, 162
 Preston, R.A., Morabito, D.D., Williams, J.G., Faulkner, J., Jauncey, D.L., & Nicolson, G.D. 1985, AJ 90, 1599
 Rees, M.J. 1967, MNRAS 137, 429
 Reynolds, S.P. 1982, ApJ 256, 13
 Sikora, M., Begelman, M.C., & Rees, M.J. 1994, ApJ 421, 153
 Thompson, D.J., et al. 1995, ApJS 101, 259
 Urry, C.M., & Padovani, P. 1991, ApJ 371, 61
 Urry, C.M., & Shafer, R.A. 1984, ApJ 280, 569
 Wagner, S.J. & Witzel, J. 1995, ARA&A 33, 163
 Zdziarski, A.A., & Krolik, J.H., 1993, ApJ 409, L33